Discharge flow of granular media from silos in presence of obstacle

S. LAIDAOUI[a,b,*], P. AUSSILLOUS[a], M. DJERMANE[b], B. DALLOZ-DUBRUJEAUD[a]

a. Aix Marseille Univ, CNRS, IUSTI, Marseille, France
b. Tahri Mohammed university of Bechar, FIMAS, BP417, Bechar 08000, Algeria
* samira.laidaoui@etu.univ-amu.fr

Résumé :

Nous présentons une étude expérimentale sur le comportement d'écoulement autour d'un obstacle cylindrique pendant la vidange de matériaux granulaires dans un silo rectangulaire. La littérature prédit que la présence d'un obstacle diminue le débit d'écoulement, mais les longueurs caractéristiques à choisir dans la loi de débit ne sont pas connues. Nous montrons que la présence de l'obstacle modifie la direction de l'écoulement. Dans cette situation, la vitesse de sortie des grains n'est plus exclusivement verticale et il est nécessaire de prendre en compte dans la loi de débit le confinement induit par la géométrie du silo rectangulaire. Pour mieux comprendre ces deux effets, une nouvelle configuration a été conçue : un silo rectangulaire avec une épaisseur réglable et une sortie dans le coin du silo.

Mots clefs : écoulement granulaire, vidange de silo.

Abstract :

We present an experimental study on the flow behaviour around a cylindrical obstacle during the discharge of granular material in a rectangular silo. As described in the literature, the presence of an obstacle decreases the flow rate, but the characteristic lengths to be chosen in the flow rate law are not known. We show that the presence of the obstacle changes the direction of the flow. In this case the confinement of the granular matter is important to take into account in the flow rate law. To better understand these two effects, a new configuration was designed, with a rectangular silo with an outlet in the corner of the silo and an adjustable thickness.

Keywords : granular flow, silo discharge.

Nomenclature

C, C_{new}, C_l	fitting parameters	
D	outlet size	m
D_{new}, D_{newc}	Characteristic lengths of the model	m
D_{obs}	obstacle diameter	m
d_p	particle diameter	m
D_x, D_y	horizontal and vertical corner outlet size	m
g	gravitational acceleration	$m.s^{-2}$
H	height of silo	m
h_O	obstacle altitude	m
L	width of silo	m
m_p	particle mass	kg
Q	discharge flow rate	$kg.s^{-1}$
Q_i	instantaneous discharge flow rate	$kg.s^{-1}$
v_0	vertical particle velocity at the outlet	$m.s^{-1}$
U_0	norm of the particle velocity at the outlet	$m.s^{-1}$
W	thickness of silo	m
Greek symbols		
α, β, γ	fitting parameters	
ρ_p	particle density	$kg.m^{-3}$
ϕ_b	bulk particle volume fraction	
ϕ_0	particle volume fraction at the centre	
θ_0	streamline angle at the centre of the outlet	

1 Introduction

Confined geometry like silos are widely used for the processing of granular and powder materials which is important in many engineering applications but the discharge flow of granular matter in silos remains an open subject of study. One of a very famous problems in silos is the jamming. A practical solution commonly implemented to solve this problem is the placement of an obstacle just above the outlet. Despite the huge number of works related to the jamming and the influence of obstacle to solve this problem [1, 2, 3, 4, 5, 6], few studies are devoted to the prediction of the discharge flow rate in the presence of an obstacle. Without obstacle, the discharge flow of a granular media from a rectangular silo, with an outlet of size D spanning the thickness, W, have been widely studied since the pioneer work of Hagen in 1852 [7] and the empirical expression proposed by Beverloo *et* al. [8]. Recently Janda *et* al. [9] have studied the flow of particles through orifices from a silo with a single layer of particles. They have found that for the whole range of apertures, the velocities profiles at the outlet are self-similar and the vertical velocity at the centre is given by $v_0 \propto \sqrt{gD}$ due to an accelerating zone which scale with the size of the orifice [10]. In the same way, the density profile was found to be self similar and the density at the centre ϕ_0 decreases with the outlet size which corresponds to a dilation of the particles at the outlet. Benyamine *et* al. [11] have shown that this dilation depends on the number of beads in the aperture D/d_p, where d_p is the particle diameter, and have proposed the following expression for the discharge flow rate, Q, from a rectangular silo:

$$Q = C\rho_p\phi_b G(\frac{D}{d_p})W D\sqrt{gD} \tag{1}$$

where the geometrical function $G(D/d_p) = (1 - \alpha e^{-\beta D/d_p}) \propto \phi_0/\phi_b$ accounts for the dilation of the beads above the aperture, ϕ_b is the bulk particle volume fraction, g the gravitational acceleration, ρ_p the particle density and C, α, β are fitting parameters.

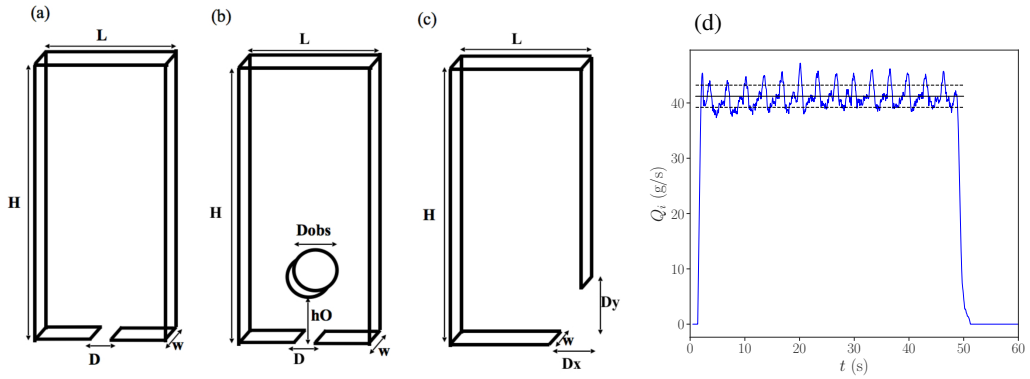

Figure 1: Different configuration of silo. (a) Outlet at the bottom without obstacle. (b) Outlet at the bottom with obstacle. (c) Outlet in the corner of silo. (d) Temporal evolution of the instantaneous mass flow rate Q_i for $d_p = 190\mu$m, $D = 12$ mm with obstacle ($D_{obs} = 20$ mm and $h_O = 5$ mm). The horizontal full line represents the mean flow rate, Q, whereas the dashed lines represent the standard deviation.

Recently Zhou *et* al. [12] have shown experimentally and using continuous simulation with a frictional rheology that if the outlet is located at a lateral position the silo thickness plays a role due to the confinement of the geometry. Indeed they have shown that the parietal friction tends to rotate the streamlines to align them toward the gravity with an angle at the outlet $sin\theta_0 \propto (1+\gamma D/W)^{-1/2}$, whereas the norm of the velocity scales with the aperture size $U_0 \propto \sqrt{gD}$. Then for large number of beads in the aperture they predicted that the flow rate follows

$$Q = C_l \rho_p \phi_b W D \frac{\sqrt{gD}}{\sqrt{1+\gamma D/W}} \tag{2}$$

where C_l and γ are fitting parameters. Thus they have observed two regimes of flow. The first regime when the aperture ratio $A = D/W$ is small corresponds to the classical Hagen law where $Q \propto W D^{3/2}$. The second regime when A is large is controlled by the confinement where $Q \propto W^{3/2} D$.

This paper is devoted to the experimental investigation of discharge flow from a rectangular silo in the presence of an obstacle. The experiments are described in section 2. Then results for the discharge flow of the silo with an obstacle are shown in section 3, and a new and more simple experimental configuration is proposed in section 4 to find out parameters which are relevant to describe the flow rate and modified the discharge flow rate law given by equation (1).

2 Experiments

All experiments have been carried out with a rectangular silo with a flat bottom (of height $H = 1100$ mm, width $L = 100$ m and thickness $W = 5$ mm). As shown in Figure 1, different configurations were designed: outlet of adjustable length D at the bottom (Fig. 1a), outlet of adjustable length D at the bottom and a cylindrical obstacle of diameter, D_{obs}, and altitude, h_0, above the outlet (Fig. 1b) and an outlet in the right bottom corner with adjustable horizontal size, D_x, and vertical size, D_y (Fig. 1c). All configurations have a free surface at the top, and the rear and front walls are made of transparent glass plates. Table 1 summarises the different parameters used for this study.

The granular material consists of smooth spherical ceramic beads of density $\rho_p = 6000$ kg/m^3 which are monodisperse in diameter with a dispersion of $\pm 20\%$ (see Table 1).

Table 1: Experimental parameters

D (mm)	D_x (mm)	D_y (mm)
12; 17.5; 24	0; 5; 10; 15; 20; 25; 30	0; 5; 10; 15; 20; 25; 30
h_O (mm)	D_{obs} (mm)	d_p (μm)
0; 5; 10; 15; 20; 30; 40	5; 10; 20; 40	190; 550; 1180; 4350

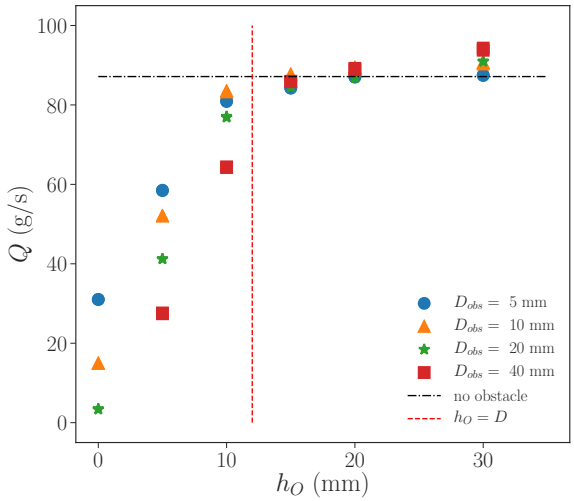

Figure 2: Mass flow rate, Q, versus the obstacle altitude, h_O, for $d_p = 190$ μm, $D = 12$ mm and various obstacle diameters D_{obs}. The horizontal dotted-dashed line represents the flow rate without obstacle. The vertical dashed line represents the altitude where $h_O = D$.

Keeping the outlet of the silo closed, a known weight m_p of ceramic beads are poured into the silo from the top. Measuring the height of the granular column, the initial bulk particle volume fraction ϕ_b is calculated for each experiment. Opening the outlet, the grains fall freely out of the silo and are collected in a vessel placed on an electronic scale with a precision of 1 g (Mettler Toledo 6002S) and the temporal evolution of the mass $m(t)$ is recorded at a frequency of 20 Hz. Each experiment is repeated twice to check the reproducibility of the process. The instantaneous mass flow rate Q_i is obtained by measuring the local slope of the temporal evolution (sliding mean value over 1 s). Figure 1d shows that in the presence of an obstacle the flow rate remains stationary, the mean flow rate Q is obtained by averaging the instantaneous flow rate over the steady state. Oscillations were observed for all experiments and have not been studied in this paper.

3 Effect of an obstacle on the discharge flow rate

First experiments were carried out with the configuration with an obstacle above the outlet (Fig. 1b). The obstacles have been positioned at different altitudes h_O above the outlet and the mean flow rate Q was measured. For a constant outlet length ($D = 12mm$) and the smallest particles ($d_p = 190$ μm), Figure 2 presents the mean flow rate versus the altitude h_O of the obstacle for various obstacle diameters D_{obs}. On this figure, the red dashed vertical line represents $h_O = D$ whereas the horizontal dotted dashed line represents the flow rate without obstacle. It is clear that the characteristic distance on which

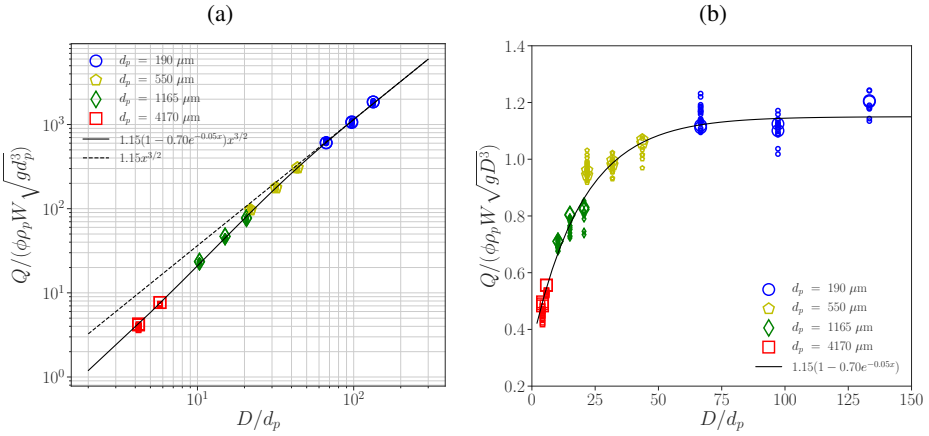

Figure 3: Mass flow rate (a) normalised by $\rho_p\phi_b W\sqrt{gd_p^3}$ and (b) normalised by $\rho_p\phi_b W\sqrt{gD^3}$ as a function of the number of beads in the aperture D/d_p for various particle diameters, and for experiments without obstacle (large symbols) and with obstacle with $h_O > D$ (small symbols). The full line represents equation 1 with $C = 1.15$, $\alpha = 0.7$ and $\beta = 0.05$. The dashed lines represent the asymptotic regime when $D/d_p >> 1$.

the obstacle modifies significantly the flow rate is for $h_O < D$. When h_O becomes smaller then D, the mass flow rate decreases, and reaches the minimum value when the obstacle touch the bottom of silo ($h_O = 0$). In this case, the mass flow rate depends of the obstacle diameter D_{obs}, the bigger the obstacle the smaller the flow rate. If $h_O > D$, the flow rate seems to stabilise and to reach the value obtained with no obstacle, whatever the obstacle diameter.

To validate this last observation, experiments were carried out with flat bottom silo without obstacle (Fig. 1a) for all particle diameters. In Figure 3(a,b) we compare the results obtained for the discharge of a silo without obstacle (large symbols) and those obtained for a silo with an obstacle placed in the area $h_O > D$ (small symbols). The flow rate is made dimensionless using the particle diameter (Fig. 3a) or the outlet size (Fig. 3b) and is plotted versus the number of beads in the aperture D/d_p. In both graph all the data collapse on a unique curve which is well fitted by equation (1) with $C = 1.15$, $\alpha = 0.70$ and $\beta = 0.05$. For small particles the Hagen law where $Q \propto DW\sqrt{gD}$ is recovered (see the dashed line in Figure 3a). This result confirms that the obstacle placed above $h_O = D$ has no influence on the discharge flow rate, which is consistent with the idea that the discharge flow rate of a silo is prescribe in an accelerating zone of typical size D, situated just above the orifice. A perturbation of the flow outside this region does not affect the flow rate. The value of the fitting parameter are in the same order of magnitude of that found for glass beads [11]. The small difference might be due to the physical properties of the beads as friction coefficients or roughness. This point is still under investigations.

When h_O becomes smaller than D, equation (1) is not valid anymore and the mass flow rate is controlled by an another length. A geometrical analysis of the outlet area with an obstacle (Fig. 4a) points out that the outlet length D is not the smallest length of the problem. We thus define a new outlet length D_{new} which is a function of D, h_0 and D_{obs}:

$$D_{new} = \sqrt{\frac{D^2}{4} + (h_O + \frac{D_{obs}}{2})^2} - \frac{D_{obs}}{2} \tag{3}$$

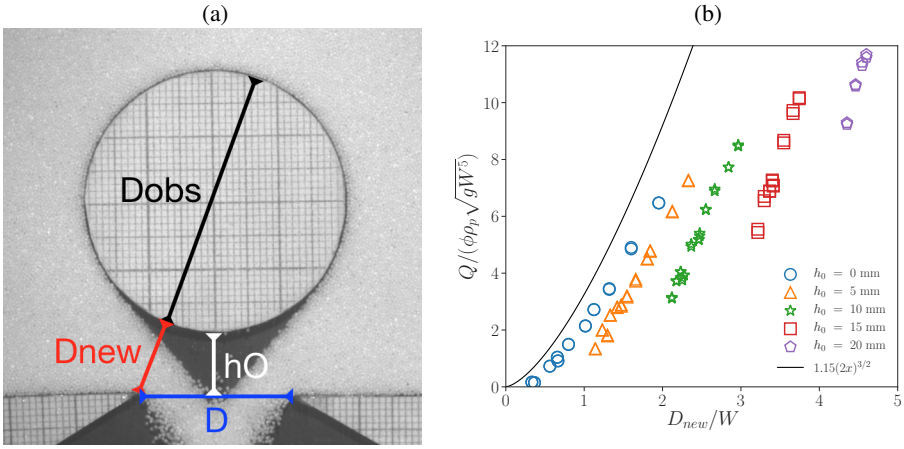

Figure 4: (a) Definition of D_{new} with in this snapshot $d_p = 550$ μm, $D = 24$ mm, $D_{obs} = 40$ mm and $h_O = 10$ mm. (b) Mass flow rate Q normalised by $\rho_p\phi_b\sqrt{gW^5}$ versus D_{new}/W for $d_p = 190$ μm and $h_O \leq D$. The full line represents the asymptotic regime of equation (1) when $D/d_p >> 1$ with $C = 1.15$ corresponding to the case without obstacle.

Figure 4b presents the normalised mass flow rate $Q/(\rho_p\phi_b\sqrt{gW^5})$ versus D_{new} normalised by the silo thickness W for the smallest particles $d_p = 190$ μm and for various obstacles altitude with $h_O \leq D$. The full line represents the asymptotic regime of equation (1) when $D/d_p >> 1$ with $C = 1.15$ corresponding to the case without obstacle. We observe that the data do not collapse and are under the prediction of equation (1) which indicates that D_{new} is not the relevant parameter.

The prediction of the mass flow rate in this configuration is complex and involves many parameters. Then to understand the parameters governing the flow rate, we propose a new and more simple configuration with an outlet in the right bottom corner (Fig. 1c). Indeed the observation of the flow around the obstacle (Fig.4a) suggests that the flow corresponds to two arms flowing out of a corner.

4 Discharge flow of a rectangular silo from a corner

This configuration allows us to control precisely the outlet with only two parameters: the horizontal and vertical extends of the aperture, respectively D_x and D_y (see Fig. 1c and Fig. 7a). We can then define a new outlet length D_{newc} given by:

$$D_{newc} = (D_x^2 + D_y^2)^{1/2} \tag{4}$$

Figure 5b presents the normalised mass flow rate versus D_{newc}/W for $d_p = 190$ μm and for the two extreme positions $D_y = 0$ (Fig. 5a) and $D_x = 0$ (Fig. 5c). We first observe that D_x and D_y do not play the same role. For an orifice at the bottom, $D_y = 0$, the flow rate is always at least 3 times higher than for a lateral orifice, $D_x = 0$, and scales on $(D_{newc}/W)^{3/2}$ as predicted by equation (1) for $D_{newc}/d_p >> 1$. To confirm this observation, experiments were carried out with all particles size in order to check the validity of the law. Results are presented on Figure 6. The normalised flow rate, using the particle diameter (Fig. 6a) or $D_{newc} = D_x$ (Fig. 6b) are in good agreement with equation 1 keeping the same α and β than for the bottom orifice situated at the centre of the silo (Fig. 1c and Fig. 3) with

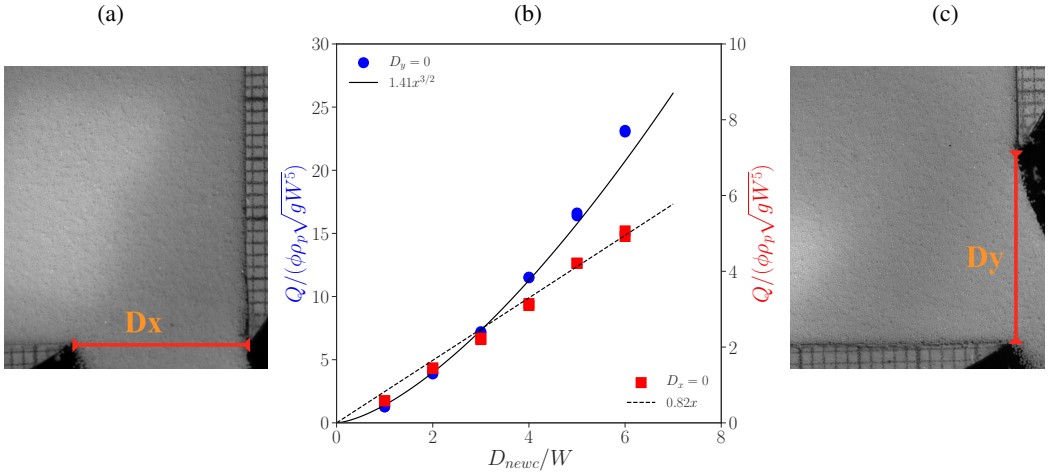

Figure 5: (a) Configuration for $D_y = 0$. (b) Mass flow rate Q normalised by $\rho_p\phi_b\sqrt{gW^5}$ versus D_{newc}/W for $d_p = 190$ μm for a bottom orifice ($D_y = 0$) and a lateral orifice ($D_x = 0$). The full line represents the asymptotic regime of equation (1) when $D/d_p >> 1$. The dashed line corresponds to the asymptotic regime of equation (2) when $D_{newc}/W >> 1$. (c) Configuration for $D_x = 0$

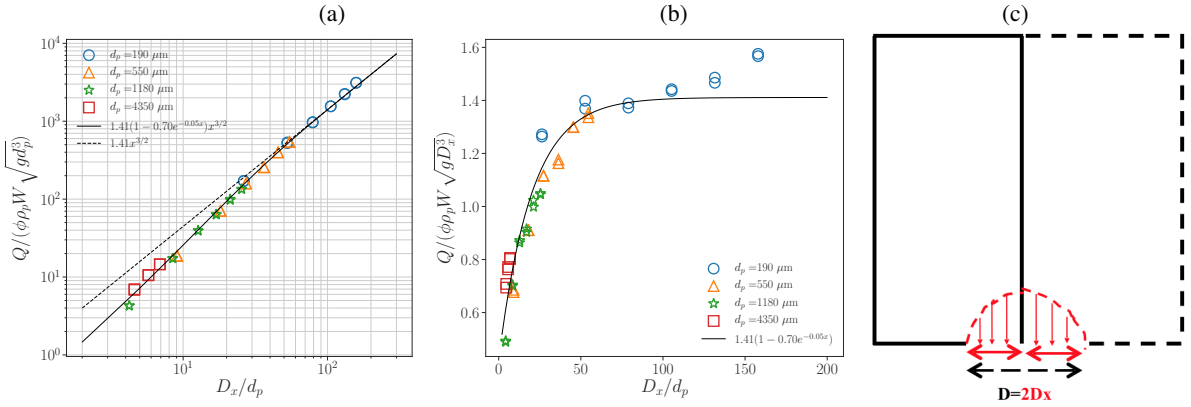

Figure 6: Mass flow rate (a) normalised by $\rho_p\phi_b W\sqrt{gd_p^3}$ and (b) normalised by $\rho_p\phi_b W\sqrt{gD^3}$ as a function of the number of beads in the aperture D_{newc}/d_p for various particle diameters and for a bottom orifice $D_y = 0$. The full line represents equation 1 with $C = 1.41$, $\alpha = 0.7$ and $\beta = 0.05$. The dashed lines represent the asymptotic regime when $D/d_p >> 1$. (c) sketch of the free slip boundary

the fitting parameter $C_{new} = 1.41$ instead of $C = 1.15$.

This difference of coefficient implies that for a bottom orifice the flow rate is higher at the border of the silo than at the centre. To understand this effect, we first consider that the vertical wall behaves as a free slip boundary. Then by symmetry, if we consider that dilation function remain similar, the flow rate will correspond to half the flow rate of an orifice of size $2D_x$ (see Fig 6c). This leads to a coefficient $C_{max} = \sqrt{2}C = 1.62$ which is the maximum value which can be observed. In our experiment the measured value lies between C and C_{max} which means that the granular media is sliding on the wall but not freely.

Considering now the case of a lateral orifice with $D_x = 0$ (Fig. 5b), two regimes are observed, the fist one for small D_{newc}/W scales with $(D_{new}/W)^{3/2}$ and the second one for larger D_{newc}/W which

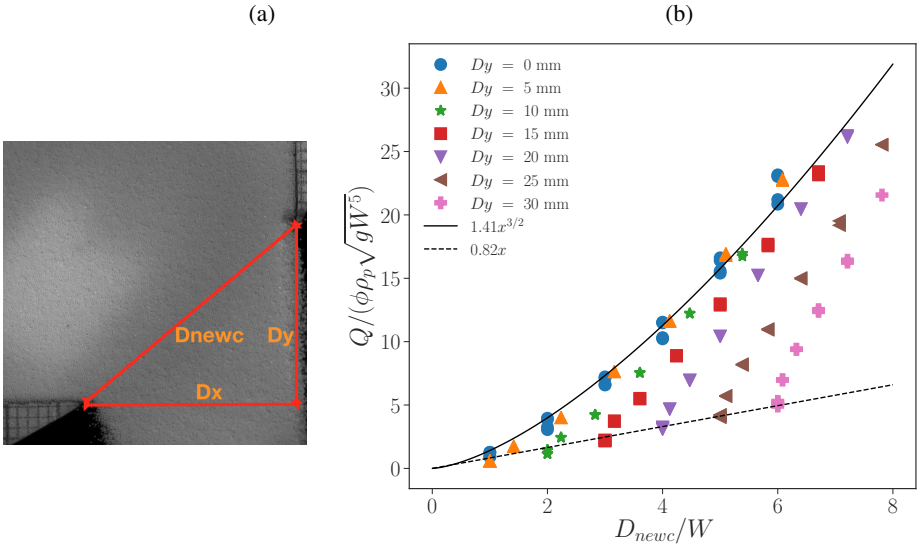

Figure 7: a) Definition of D_{newc} with in this snapshot $d_p = 190$ μm, $D_x = 25$ mm and $D_y = 20$ mm. (b) Mass flow rate Q normalised by $\rho_p \phi_b \sqrt{gW^5}$ versus D_{newc}/W for $d_p = 190$ μm and $h_O \leq D$. The full line represents the asymptotic regime of equation (1) when $D/d_p >> 1$ with $C = 1.41$ (case $D_y = 0$). The dashed line represents the asymptotic regime of equation (2) when $D_{newc}/W >> 1$ (case $D_x = 0$).

is linear with D_{newc}/W (dashed line). These results are in good agreement with the experimental and numerical results of Zhou et al. [12]. This shows that the silo thickness is also an important parameter of control of the discharge flow from a corner, due to the friction on the front and rear wall. The transition between this two regimes depends on the ratio (D_y/W). Some more experiments will be carried out for a larger silo in order to change the value of W and characterise the transition for ceramic beads.

When D_x and D_y are non-zero values, all our results are in between these two regimes as we can see on Figure 7b which presents the normalised mass flow rate $Q/(\rho_p \phi_b \sqrt{gW^5})$ versus D_{newc}/W for $h_O \leq D$. This figure shows that D_{newc} is not the correct parameter to describe the discharge flow rate from a corner. However varying D_y we observe the same trend than varying h_O in the presence of an obstacle (Fig. 4b) which gives support to the analogy between the flow around an obstacle and the flow through a corner. Further work will be done experimentally (particle image velocimetry on the images and varying the thickness of the silo) and numerically (continuous simulation using a granular rheology) to better understand the physical process and the relevant parameters.

5 Conclusion

We have experimentally studied the discharge flow of ceramic beads from a rectangular silo in the presence of a cylindrical obstacle. We have shown that for an altitude higher than the orifice length the obstacle does not infer on the flow rate, while when situated in the zone of acceleration above the outlet the presence of the obstacle decreases significantly the flow rate. We have shown that the flow rate depends on all the parameters varied: the outlet size, the obstacle position and diameter, and possibly the silo thickness and the particle diameters. Using the minimum distance between the obstacle and the silo does not allow to scale the data. To simplify the problem we have experimentally studied the

discharge flow of ceramic beads from a rectangular silo from a corner. We have shown that for a bottom orifice at the wall the flow rate obeys the same law than in the centre (equation 1), with a slightly higher coefficient due to the boundary condition at the wall. For a lateral orifice we observe two regimes of flow (equation 2) where for large aperture and narrow silo the flow is dominated by the parietal friction and depends on the silo thickness. For the corner, we observe that all the data are in between these two cases, which suggest that the silo thickness is indeed a parameter which has to be taken into account in the discharge flow from a corner or in the presence of an obstacle. To better understand the physical process and the relevant parameters, future works will be devoted to the study of particle velocities using image processing and the thickness of the silo will be varied.

Acknowledgments

S. L. thanks Bechar University, Aix-Marseille University, IUSTI laboratory and Franco-Algerian program Profas B+ for support. This work was undertaken under the auspices of the Labex MEC (ANR-10-LABX-0092) and of the A*MIDEX project (ANR-11-IDEX-0001-02), funded by the Investissements d'Avenir program managed by the French National Research Agency (ANR).

References

[1] J.R. Johanson, The use of flow corrective inserts in bins, *J. Eng. for Ind.* 2 (1966) 224-230.

[2] J.R. Johanson, The placement of inserts to correct flow in bins, *Powder Technol.* 1 (1967/68) 328-333.

[3] R.M. Nedderman, S.T. Davies and D.J. Horton, The flow of granular materials round obstacles, *Powder Technol.* 25 (1980) 215-223.

[4] U. Tuzun and R.M. Nedderman, Gravity flow of granular materials round obstacles-I: Investigation of the effects of inserts on flow patterns inside a silo, *Chem. Eng. Sci* 40(3) (1985) 325-336.

[5] I. Zuriguel, A. Janda, A. Garcimartin, C. Lozano, R. Arevalo, D. Maza, Silo clogging reduction by the presence of an obstacle, *Phys. Rev. Lett.* 107 (2011) 278001.

[6] C. Lozano, A.Janda, A. Garcimartin, D . Maza, I. Zuriguel, Flow and clogging in a silo with an obstacle above the orifice, *Phys. Rev. E*, 86 (2012) 031306.

[7] B. P. Tighe and M. Sperl, Pressure and motion of dry sand: translation of Hagen's paper from 1852, *Granular Mat.* , 9 (2007) 141-144.

[8] W.A. Beverloo, H.A. Leniger and J.V. De Velde, The flow of granular solids through orifices, *Chem. Eng. Sci.* 15 (1961) 260-269.

[9] A. Janda, I. Zuriguel and D. Maza, Flow rate of particles through apertures obtained from self-similar density and velocity profiles, *Phys. Rev. Lett.* 108 (2012) 248001.

[10] S. Rubio-Largo, A. Janda, D. Maza, I. Zuriguel and R. Hildalgo, Disentangling the free-fall arch paradox in silo discharge, *Phys. Rev. Lett.* 114 (2015) 238002 .

[11] M. Benyamine, M. Djermane, B. Dalloz-Dubrujeaud and P. Aussillous, Discharge flow of a bidisperse granular media from a silo, *Phys. Rev. E*, 90 (2014) 032201 .

[12] Y. Zhou, P.-Y. Lagrée, S. Popinet, P. Ruyer, P. Aussillous, Experiments on, and discrete and continuum simulations of, the discharge of granular media from silos with a lateral orifice, *J. Fluid Mech.*, 829 (2017) 459-485.